Faithful Solid State Optical Memory with Dynamically Decoupled Spin Wave Storage

Marko Lovrić,[1,2,*] Dieter Suter,[1] Alban Ferrier,[2] and Philippe Goldner[2,†]

[1]Technische Universität Dortmund, Fakultät Physik, D-44221 Dortmund, Germany
[2]Chimie ParisTech, Laboratoire de Chimie de la Matière Condensée de Paris, CNRS-UMR 7574, UPMC-Paris 06, 11 rue Pierre et Marie Curie 75005 Paris, France

(Received 14 February 2013; published 11 July 2013)

We report a high fidelity optical memory in which dynamical decoupling is used to extend the storage time. This is demonstrated in a rare-earth doped crystal in which optical coherences were transferred to nuclear spin coherences and then protected against environmental noise by dynamical decoupling, leading to storage times of up to 4.2 ms. An interference experiment shows that relative phases of input pulses are preserved through the whole storage and retrieval process with a visibility ≈ 1, demonstrating the usefulness of dynamical decoupling for extending the storage time of quantum memories. We also show that dynamical decoupling sequences insensitive to initial spin coherence increase retrieval efficiency.

DOI: 10.1103/PhysRevLett.111.020503 PACS numbers: 03.67.Lx, 32.80.Qk, 42.50.Md, 76.30.Kg

Quantum memories for light (QML) are devices capable of faithfully storing photonic quantum states into atomic states [1]. Their applications include long distance quantum cryptography and, more generally, quantum networks [2]. Besides atomic vapors, rare-earth ions have recently been considered as promising candidates for solid state QMLs. This is because of the coherence lifetimes of their optical and nuclear spin transitions, which can reach the ms range [3,4]. Moreover, these systems are well suited for memories with large time-bandwidth products since their optical inhomogeneous linewidth can exceed by several orders of magnitude the homogeneous one [3]. To take advantage of this property, the optical input signal is absorbed in an inhomogeneously broadened transition. Excited atomic coherences then dephase and, after a time t, are rephased by an optical control pulse, resulting in an output signal at time $2t$ similar to a photon echo [5]. Protocols like controlled reversible inhomogeneous broadening [6], gradient echo memory [7], atomic frequency comb (AFC) [8,9] or revival of silenced echo [10] have been developed from this basic scheme to allow for high efficiency, high bandwidth, and single photon level input signals. To reach long storage times, the optical coherence can be transferred to a ground state nuclear spin coherence. This is also required in the AFC protocol to obtain an on-demand memory [11]. Using these protocols in different rare-earth crystals, recent demonstrations include 1 GHz bandwidth storage [12], 70% storage efficiency [13], entanglement storage [14,15], and entanglement of two crystals [16]. Transfer to spin states has also been reported, although storage times were limited to 20–50 μs [11,17,18] because of the lack of spin refocusing. On the other hand, long storage times, up to several seconds, have been observed using electromagnetically induced transparency [19–21]. This was achieved by controlling rare-earth spin decoherence with a combination of external magnetic fields [22,23] and dynamical decoupling (DD) with radio-frequency (rf) pulses [24,25]. These storage times are comparable to those obtained in atomic vapors [26,27]. Along with storage time, efficiency, and bandwidth, fidelity is also a crucial point for optical quantum memories. In several systems, high fidelity storage has been deduced from comparison between input and output light states using interference [28,29] or polarization analysis [30,31], depending on the photonic quantum state. In particular, time bin optical pulses were stored with a fidelity of $\approx$1 using a stimulated photon echo scheme [32].

Here, we provide the first demonstration of high fidelity storage in an ensemble-based optical memory which uses DD. The memory consists of a rare-earth doped crystal in which the optical coherence is transferred to a nuclear spin coherence and further controlled by rf DD sequences. We show that relative optical phases are preserved with a fidelity close to 1, indicating the high potential of DD for ensemble-based optical memories in general. This technique allowed us to achieve storage times up to 4.2 ms, corresponding to a 33-fold increase in spin wave storage time over the intrinsic spin coherence lifetime. Comparison between DD sequences also reveals that sequences insensitive to initial spin coherence increase retrieval efficiency.

Experiments were performed on a 0.2 at. % Pr^{3+}:$La_2(WO_4)_3$ single crystal. This material was developed for quantum memories to reach low optical inhomogeneous broadening at high Pr^{3+} concentration in order to increase optical depth [33,34]. The crystal was cooled down to a temperature of $\approx$ 5 K in a cold finger liquid helium cryostat. Optical excitation was provided by a Coherent 899-21 dye laser stabilized to a linewidth $<$20 kHz using a high finesse cavity and a home-built Pound-Drever-Hall stabilization setup [35]. Light propagated parallel to the crystal b axis and was focused to a spot of 40 μm inside the sample which was 4 mm thick. The maximum laser power incident on the crystal was 100 mW (8 kW/cm^2 intensity). Optical pulse amplitude

and frequency were controlled by acoustic-optic modulators in double pass configuration, driven by an arbitrary waveform generator. The signal was detected by an avalanche photodiode. To apply rf pulses, a 6 mm, 10 turn coil surrounded the crystal. To reduce reflections and increase the field strength, the coil was part of a tuned circuit, which was driven with maximum rf power of 9 W and controlled by a 300 MS/s direct digital synthesizer. Optical excitations were resonant with transitions between the lowest electronic level of the Pr^{3+} $^3H_4$ ground and the $^1D_2$ excited state multiplet (Fig. 1, upper part). The optical transition has a peak absorption coefficient of 3.5 cm^{-1}, an inhomogeneous linewidth of 10 GHz and a homogeneous one of 27 kHz ($T_2 = 11.5$ μs). $^{141}Pr^{3+}$ has a $I = 5/2$ nuclear spin and 100% abundance. Each electronic level has a hyperfine structure of three doubly degenerate levels (Fig. 1, upper part) at zero external magnetic field. The strongest optical transition occurs between levels (i) and (e) [36] and was chosen to absorb the input signal. Spin storage was performed on the (i)–(t) transition at 14.87 MHz.

As the optical inhomogeneous linewidth is much larger than the hyperfine level separation, optical pumping with the narrow linewidth laser was first used to isolate the transitions of interest. The first step of the optical pumping

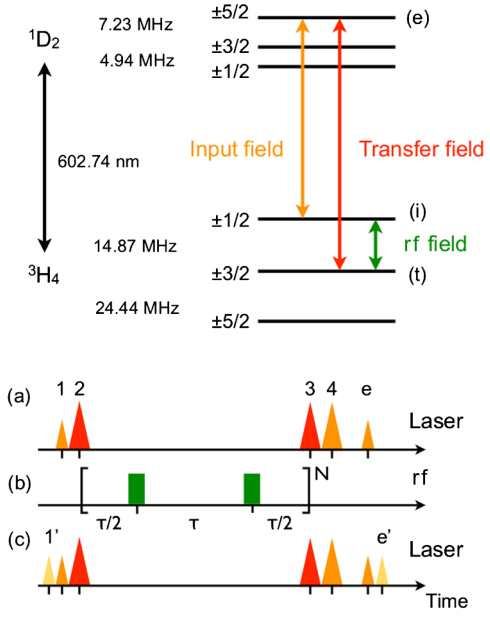

FIG. 1 (color online). Upper part: hyperfine structure of Pr^{3+} $^3H_4$ and $^1D_2$ levels in Pr^{3+}:$La_2(WO_4)_3$ and transitions used in this Letter. Lower part: laser sequences for one (a) or two (c) pulse storage. Pulses 1 and 4 were Gaussian with full width at half maximum (FWHM) lengths of 200 and 425 ns, respectively. Pulses 2 and 3 were secant hyperbolic with FWHM length of 2.25 μs and a 2 MHz chirp. The delay t_{12}, between pulse 1 and 2, and t_{34} were set to 2 μs. Comparing echo intensity with and without transfer pulses, we deduced a transfer efficiency for fields of 87% per pulse. (b) rf pulse sequence for hyperfine transition dynamical decoupling; the basic block showed in brackets is repeated N times (see text).

sequence [36] consisted in burning a spectral pit of 25 MHz, to empty levels (i) and (t) for one class of ions. Population was then brought back into the (i) level of these ions by a pulse adjusted to create a 1.5 MHz wide absorption peak. Finally, additional pulses were applied to remove unwanted spectral features in the pit. Figure 2 shows the final transmission spectrum at the end of the preparation sequence. It consists of a well isolated peak at 12.2 MHz corresponding to the (i)–(e) transition and a low background absorption on the (t)–(e) transition at 27.0 MHz. Level (t) is, therefore, empty, which is required for efficient transfer of the optical (i)–(e) coherence to the hyperfine (i)–(t) transition.

Figures 1(a) and 1(b) show the general memory sequence that we used. The input signal (pulse 1) was first absorbed by the inhomogeneously broadened (i)–(e) transition. The resulting coherence was then transferred to the hyperfine (i)–(t) coherence by a π pulse resonant with the (t)–(e) transition (pulse 2). The inhomogeneous dephasing of the resulting initial spin coherence was refocused by an even number of rf π pulses applied to the (i)–(t) transition [see Fig. 1(b)]. If the pulses are applied at a rate larger than the correlation time of the dephasing bath, the spin transition coherence lifetime may increase through DD [37]. This is because the bath appears static, like an additional inhomogeneous broadening, between successive π pulses. The rf pulses refocus this broadening and effectively increase the transition coherence lifetime. Ideally, after the last rf pulse and a delay of $\tau/2$, where τ is the rf pulse separation, the hyperfine coherence state is the same as the initial one. Applying a second transfer at this time (pulse 3) brings the hyperfine coherence back to the optical domain. A final π pulse along the (i)–(e) transition (pulse 4), refocuses the optical dephasing of the coherence. Finally, the output signal (pulse e) appears as a photon echo at a time $t_{4e} = t_{12} + t_{34}$ after pulse 4, where t_{ij} is the delay between pulses i and j. The memory storage time is $T = t_{1e}$.

rf pulses of rectangular shape were applied between the transfer pulses as shown in Figs. 1(a) and 1(b). Using

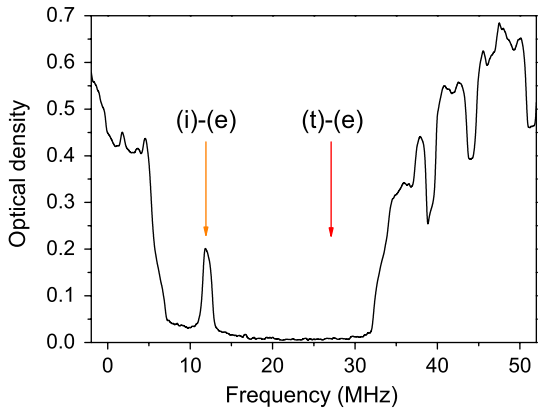

FIG. 2 (color online). Absorption spectrum after optical pumping.

an appropriate rf power, the pulse area was set to π, while their duration was set to 5 μs so that their spectral width ($\approx$200 kHz) was larger than the inhomogeneous linewidth of the (i)–(t) transition (45 kHz). The pulse amplitude was determined by nutation and spin echo experiments. The relative phase of successive rf pulses could be adjusted, X and Y representing, respectively, 0° and 90° phases in the following. The optical phase of the laser was independent of the rf phase; thus, for each repetition of the experiment the initial phase of the spins was arbitrary compared to the rf pulse phases. Moreover, since the first transfer pulse was applied after evolution in the optical domain, there was a distribution of initial spin phases. As a result, no spin echo was observed between rf pulses or at the end of the rf sequence. Only the final optical echo could be used to probe the spin coherence decay. The rf sequences consisted of a basic block of length 2τ, which was repeated N times [see Fig. 1(b)].

We compared two DD sequences. Their building blocks, where $\pi(\phi)$ represents a rf π pulse with ϕ phase, are given by (i) $[\tau/2 - \pi(X) - \tau - \pi(X) - \tau/2]$, Carr-Purcell-Meiboom-Gill (CPMG) sequence [38]; (ii) $[\mathrm{KDD}(X) - \mathrm{KDD}(Y) - \mathrm{KDD}(X) - \mathrm{KDD}(Y)]$, where $\mathrm{KDD}(\phi) = [\tau/2 - \pi(\phi + \pi/6) - \tau - \pi(\phi) - \tau - \pi(\phi + \pi/2) - \tau - \pi(\phi) - \pi(\phi + \pi/6) - \tau/2]$, Knill DD (KDD) sequence [39]. The CPMG sequence has one of the highest decoupling efficiencies, but only when the spins are initially aligned with the rotation axis of the pulses [40]. The KDD sequence is designed to be insensitive to initial phases [39].

Figure 3 shows the output signal intensity I as a function of the storage time T for the CPMG and KDD sequences. I is normalized to the output pulse obtained with zero delay between transfer pulses and no rf pulses, and is plotted as a retrieval efficiency. The pulse separation τ was 30 μs for KDD and CPMG sequences and was optimized for the longest storage time with KDD. As shown in Fig. 3, output signal decays were approximately exponential resulting in $1/e$ storage times of 4.2 and 0.95 ms for CPMG and KDD sequences, respectively. The corresponding effective coherence lifetimes $T_{2,\mathrm{eff}}$ were 8.4 and 1.9 ms. Compared to using only 2 rf pulses ($T_{2,\mathrm{eff}} = 230$ μs), i.e., refocusing only the static inhomogeneous spin broadening, the two DD sequences significantly increase the storage time $T_{2,\mathrm{eff}}$ (see Fig. 3). A signal to noise ratio of 2 after 200 accumulations is reached at a storage time $T = 20$ ms for CPMG and at $T = 7$ ms for KDD. CPMG provides the longest relaxation time, since it 'locks' the spins along the effective field generated by the pulses. However, at 300 μs storage time, KDD's retrieval efficiency is nearly twice the one obtained with CPMG (12% and 6.4%, respectively). This can be explained by the initial distribution of spin phases at the input of the DD sequences (see above): CPMG preserves only the component of the spin which is initially oriented along the rotation axis of the pulses, while KDD protects all spin components and, therefore, the full quantum state, as required for a quantum memory [39].

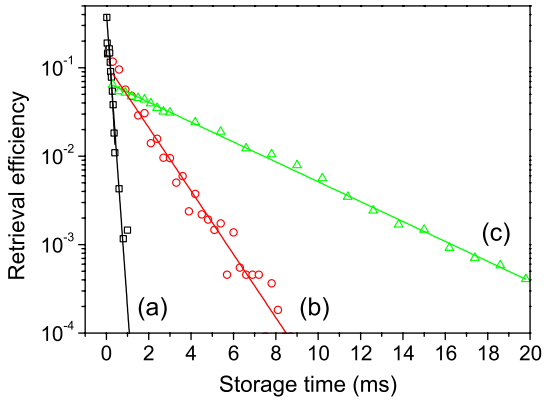

FIG. 3 (color online). Retrieval efficiency as a function of storage time using two rf pulses (a), KDD (b), and CPMG (c) dynamical decoupling sequences. The retrieval efficiency is normalized to the echo intensity extrapolated at zero delay, using transfer pulses but no rf pulses.

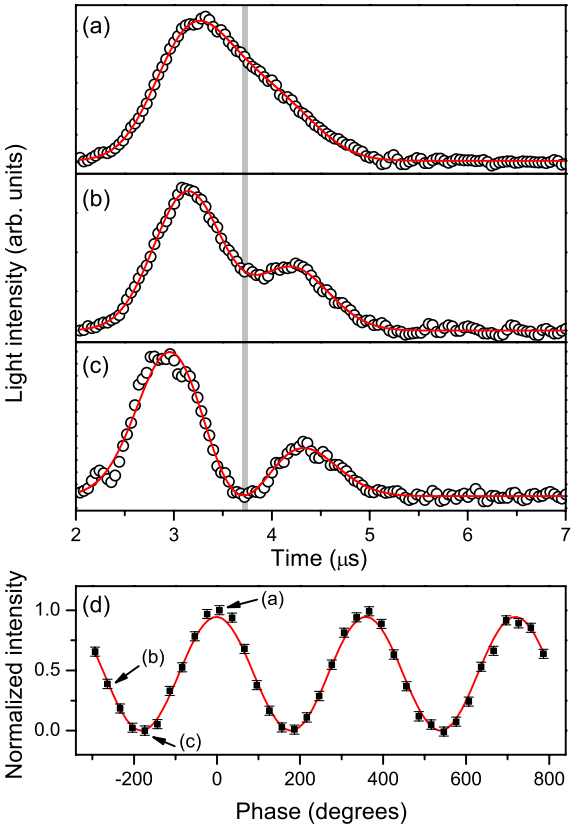

FIG. 4 (color online). Interfering output pulses after storage of two input pulses, with 0° (a), −270° (b), and −180° (c) relative phases, for 3 ms. Open circles: experimental data, solid line: fit using two Gaussian pulses. (d) Normalized output light intensity averaged at 3.7 μs over 50 ns [gray area in (a)–(c)] as a function of the relative input pulse phase. Squares: experimental data, solid line: fit with a visibility expression (see text).

Finally, we checked the fidelity of the memory by storing two optical pulses [32,41]. As the laser coherence lifetime is only about 50 μs, the phase of the output pulses from identically repeated experiments are random. Therefore, only relative phases between successive input and output pulses (within $\approx$50 μs) are relevant. The sequence used is shown in Figs. 1(c) and 1(b). Compared to sequence (a), an additional Gaussian pulse (pulse $1'$) of 200 ns FWHM duration is stored in the memory with a delay $t_{1'1} = 1$ μs. The rf DD sequence followed the KDD scheme with $\tau = 30$ μs and a storage time of 3 ms. As the spectral width of the input pulses was about 5 MHz, but the prepared absorption line [(i)–(e), see Fig. 2] was only 1.5 MHz wide, the output pulses e and e' were broadened to 400 ns and, therefore, overlapped in time and interfered. Figs. 4(a)–4(c) show the overlapping output pulses when the relative phase of the input pulses is 0°, −270°, and −180°, respectively. The output intensities were well modeled by two overlapping Gaussian pulses [see Figs. 4(a)–4(c)], confirming the origin of the output signal variations. Light intensity was then averaged over 50 ns around the center of the interfering region [see Figs. 4(a)–4(c)] and normalized. This intensity $I_n(\phi)$ is plotted against the input pulses relative phase ϕ in Fig. 4(d) and was well fitted by the visibility expression $I_n(\phi) = (I_{\max}/2)[1 + V\sin(\phi)]$ with $V = 0.99$. Therefore, relative phases are preserved through the whole storage process, which is a key requirement for a quantum memory. Similar results were obtained with the CPMG sequence with storage times up to 10 ms.

In conclusion, we have demonstrated a high fidelity light storage in a rare-earth doped crystal where storage times are extended through DD. This was shown by storing two input pulses which are allowed to interfere at the output of the memory. This key property allows considering application of DD techniques to extend storage times of ensemble-based quantum memories. Depending on the decoupling sequence, storage times between 0.95 and 4.2 ms have been achieved together with an optical bandwidth of 1.5 MHz, corresponding to a maximum time-bandwidth product of 6.3×10^3. We also found that decoupling sequences insensitive to initial spin states, such as KDD, increase the retrieval efficiency.

The authors thank Mikael Afzelius for useful discussions. This work was supported by the European Union FP7 Projects QuRep (No. 247743) and CIPRIS (Marie Curie Action No. 287252).

*Present address: Sirah Lasertechnik GmbH, Heinrich-Hertz-Straße 11, D-41516 Grevenbroich, Germany.
†philippe-goldner@chimie-paristech.fr

[1] A. I. Lvovsky, B. C. Sanders, and W. Tittel, Nat. Photonics **3**, 706 (2009).
[2] H. J. Kimble, Nature (London) **453**, 1023 (2008).
[3] R. M. Macfarlane, J. Lumin. **100**, 1 (2002).
[4] A. L. Alexander, J. J. Longdell, and M. J. Sellars, J. Opt. Soc. Am. B **24**, 2479 (2007).
[5] W. Tittel, T. Chanelière, R. L. Cone, S. Kröll, S. A. Moiseev, and M. J. Sellars, Laser Photonics Rev. **4**, 244 (2010).
[6] M. Nilsson and S. Kröll, Opt. Commun. **247**, 393 (2005).
[7] G. Hétet, J. J. Longdell, A. L. Alexander, P. K. Lam, and M. J. Sellars, Phys. Rev. Lett. **100**, 023601 (2008).
[8] H. de Riedmatten, M. Afzelius, M. U. Staudt, C. Simon, and N. Gisin, Nature (London) **456**, 773 (2008).
[9] M. Afzelius, C. Simon, H. de Riedmatten, and N. Gisin, Phys. Rev. A **79**, 052329 (2009).
[10] V. Damon, M. Bonarota, A. Louchet-Chauvet, T. Chanelière, and J.-L. Le Gouët, New J. Phys. **13**, 093031 (2011).
[11] M. Afzelius, I. Usmani, A. Amari, B. Lauritzen, A. Walther, C. Simon, N. Sangouard, J. Minář, H. de Riedmatten, N. Gisin, and S. Kroll, Phys. Rev. Lett. **104**, 40503 (2010).
[12] M. Bonarota, J.-L. Le Gouët, and T. Chanelière, New J. Phys. **13**, 013013 (2011).
[13] M. P. Hedges, J. J. Longdell, Y. Li, and M. J. Sellars, Nature (London) **465**, 1052 (2010).
[14] C. Clausen, I. Usmani, F. Bussières, N. Sangouard, M. Afzelius, H. de Riedmatten, and N. Gisin, Nature (London) **469**, 508 (2011).
[15] E. Saglamyurek, N. Sinclair, J. Jin, J. A. Slater, D. Oblak, F. Bussières, M. George, R. Ricken, W. Sohler, and W. Tittel, Nature (London) **469**, 512 (2011).
[16] I. Usmani, C. Clausen, F. Bussières, N. Sangouard, M. Afzelius, and N. Gisin, Nat. Photonics **6**, 234 (2012).
[17] M. Gündoğan, M. Mazzera, P. M. Ledingham, M. Cristiani, and H. de Riedmatten, New J. Phys. **15**, 045012 (2013).
[18] N. Timoney, I. Usmani, P. Jobez, M. Afzelius, and N. Gisin, arXiv:1301.6924v1.
[19] M. Fleischhauer, A. Imamoglu, and J. Marangos, Rev. Mod. Phys. **77**, 633 (2005).
[20] J. J. Longdell, E. Fraval, M. J. Sellars, and N. B. Manson, Phys. Rev. Lett. **95**, 063601 (2005).
[21] G. Heinze, A. Rudolf, F. Beil, and T. Halfmann, Phys. Rev. A **81**, 011401 (2010).
[22] E. Fraval, M. J. Sellars, and J. J. Longdell, Phys. Rev. Lett. **92**, 077601 (2004).
[23] M. Lovrić, P. Glasenapp, D. Suter, B. Tumino, A. Ferrier, P. Goldner, M. Sabooni, L. Rippe, and S. Kröll, Phys. Rev. B **84**, 104417 (2011).
[24] E. Fraval, M. J. Sellars, and J. J. Longdell, Phys. Rev. Lett. **95**, 030506 (2005).
[25] M. F. Pascual-Winter, R. C. Tongning, T. Chanelière, and J.-L. Le Gouët, Phys. Rev. B **86**, 184301 (2012).
[26] R. Zhang, S. R. Garner, and L. V. Hau, Phys. Rev. Lett. **103**, 233602 (2009).
[27] Y. O. Dudin, L. Li, and A. Kuzmich, Phys. Rev. A **87**, 031801 (2013).
[28] Y.-H. Chen, M.-J. Lee, I.-Chung Wang, S. Du, Y.-F. Chen, Y.-C. Chen, and I. A. Yu, Phys. Rev. Lett. **110**, 083601 (2013).
[29] K. F. Reim, J. Nunn, V. O. Lorenz, B. J. Sussman, K. C. Lee, N. K. Langford, D. Jaksch, and I. A. Walmsley, Nat. Photonics **4**, 218 (2010).
[30] H. Gao, M. Rosenberry, and H. Batelaan, Phys. Rev. A **67**, 053807 (2003).

[31] C. Clausen, F. Bussières, M. Afzelius, and N. Gisin, Phys. Rev. Lett. **108**, 190503 (2012).
[32] M. U. Staudt, S. R. Hastings-Simon, M. Nilsson, M. Afzelius, V. Scarani, R. Ricken, H. Suche, W. Sohler, W. Tittel, and N. Gisin, Phys. Rev. Lett. **98**, 113601 (2007).
[33] F. Beaudoux, O. Guillot-Noël, J. Lejay, A. Ferrier, and P. Goldner, J. Phys. B **45**, 124014 (2012).
[34] P. Goldner, O. Guillot-Noël, F. Beaudoux, Y. Le Du, J. Lejay, T. Chanelière, J. L. Legouet, L. Rippe, A. Amari, A. Walther, and S. Kröll, Phys. Rev. A **79**, 033809 (2009).
[35] R. W. P. Drever, J. L. Hall, F. V. Kowalski, J. Hough, G. M. Ford, A. J. Munley, and H. Ward, Appl. Phys. B **31**, 97 (1983).
[36] O. Guillot-Noël, P. Goldner, F. Beaudoux, Y. Le Du, J. Lejay, A. Amari, A. Walther, L. Rippe, and S. Kröll, Phys. Rev. B **79**, 155119 (2009).
[37] L. Viola and S. Lloyd, Phys. Rev. A **58**, 2733 (1998).
[38] S. Meiboom and D. Gill, Rev. Sci. Instrum. **29**, 688 (1958).
[39] A. M. Souza, G. Álvarez, and D. Suter, Phys. Rev. Lett. **106**, 240501 (2011).
[40] A. M. Souza, G. A. Álvarez, and D. Suter, Phil. Trans. R. Soc. A **370**, 4748 (2012).
[41] M. Lovrić, Ph.D. thesis, Technical University of Dortmund (2012).